Thermal Bridging and its Mitigation in Bamboo Panel Construction with Steel Frameworks and Mineral Wool Insulation

Haidong Li,[a] Wenjun Zhang,[a] Yunxing Zhang,[a] Feifei Zhai,[a,*] and Fuming Chen [b,*]

An energy-efficient and environmentally conscious bamboo-constructed residential structure was created, comprising bamboo composite panels, steel framework, and mineral wool insulation. To ascertain the efficacy of this particular type of wall in enhancing thermal capabilities, the finite element method was employed to analyze the factors influencing the thermal performance of the exterior wall panels, insulation layer, framework, and interior wall panels. A more judicious design and implementation strategy, known as the 3# and 8# combination scheme, was evaluated in practical applications to assess the thermal efficiency of the wall system. The findings indicated that augmenting the thickness of the inner and outer wall panels and insulation layer, reducing the framework thickness, and incorporating wooden framework as a substitute for steel framework within a certain range enhanced the thermal capabilities of bamboo-constructed walls and mitigated the adverse effects of thermal bridges. The thermal performance of the residences employing the newly developed bamboo-constructed walls surpassed that of conventional iron container houses, thereby warranting broader adoption and application in practical projects. These outcomes offer valuable insights for the optimized design of thermal performance in bamboo-constructed walls.

DOI: 10.15376/biores.19.1.416-433

Keywords: ANSYS; Bamboo wall; Numerical simulation; Heat transfer coefficient; Thermal bridge effect

Contact information: a: School of Architectural and Artistic Design, Henan Polytechnic University, Jiaozuo, Henan, 454000, P.R. China; b: International Centre for Bamboo and Rattan, 8 FuTong Eastern Avenue, Wangjing Area, Chaoyang District, Beijing 100102, P.R. China;
** Corresponding authors: lkyzff@163.com; chenfuming1985@126.com*

INTRODUCTION

Industrial energy consumption, building energy consumption, and transportation industry energy consumption are the primary facets of overall societal energy consumption. Among these, energy consumption of buildings during the operation (heating and cooling) of buildings has become the main growth point of energy consumption (Huo *et al*. 2017; Yan *et al*. 2017), garnering increasing scrutiny. The building wall material constitutes approximately 70% of the entire house construction material, thus assuming a pivotal role in fostering energy efficiency. Bamboo, as an engineering material, is being promoted as a lightweight, high-strength, and exceptionally thermally insulating building material, thereby holding immense significance in augmenting wall insulation performance while curbing building energy consumption. Consequently, it has attracted mounting attention from scholars.

The exploration of composite bamboo walls encompasses investigations into their physical-mechanical and thermal attributes, with a greater abundance of studies focusing on the former. The thermal insulation properties of walls boasting varying structural layer thicknesses have been examined (Chen *et al*. 2013; Zhou *et al*. 2019). The performance of steel-bamboo composite wall structures has been evaluated, reaffirming their exceptional seismic, flexural, heat transfer, and carbon reduction capabilities (Li *et al*. 2015, 2017; Shan *et al*. 2020). In the realm of joint design properties, Trujillo and Malkowska (2018) utilized a wood engineering experimental method to ascertain three key attributes (namely, locating nail embedment strength, slip modulus, and screw retraction capacity) for 151 bamboo species. Lv *et al*. (2019) scrutinized the thermal insulation performance of walls crafted from novel engineered cross-laminated bamboo (CLB) and observed that enhanced thermal insulation performance correlated with increased wall thickness. However, they noted that different wall configurations had minimal impact on thermal insulation performance when maintaining the same wall thickness. Zhou *et al*. (2023) conducted a comprehensive exploration of the parameters influencing the axial compression performance of walls employing bamboo fiber reinforced phosphogypsum composites, culminating in the proposal of a combined wall axial approach. Moreover, Huang and Sun (2021) substantiated the viability of employing multilevel comparisons for bamboo units, specifically regarding their hygrothermal performance. While research on the thermal performance of bamboo walls remains incomplete, further investigations into optimizing thermal insulation capabilities are still imperative.

Diverse methodologies exist for investigating the thermal performance of walls, encompassing experimental tests, finite element simulation, and mathematical calculation analysis. A simple linear calculation method can well estimate the heat flux at each point perpendicular to the wall surface and provide a reasonable initial estimate. In addition, it can also be used as a method to test the effectiveness of sector calculation. Liu *et al*. (2022) harnessed the power of ABAQUS finite element software to conduct numerical simulations, analyzing the thermal performance of blocks and walls adorned with various insulation materials. Zhou *et al* (2020) ingeniously constructed a wall composed of ribbed beams and ribbed columns, embellished with straw panels arranged in a lattice-like frame, subsequently employing calibrated hot box experimental methods to numerically simulate the one-dimensional steady-state heat transfer within said wall via the aid of ABAQUS finite element software. Alghamdi and Alharthi (2017) fashioned autoclaved aerated concrete (AAC) panels of varying densities and thicknesses, fashioning a composite sandwich wall utilizing AAC and calcium silicate board (CSB). They simulated the temperature field and calculated heat transfer coefficients using ANSYS software, substantiating their research. Yang *et al.* (2023) meticulously examined the impact of slotted webs on the thermal performance of composite walls, featuring light steel studs, employing a combination of calibrated hot box experiments and ANSYS finite element simulations. Zhai *et al*. (2018) employed an ANSYS finite element model to scrutinize the influence of parameters such as wrapped nylon, thermal conductivity, connector spacing, central reinforcement diameter, and insulation thickness on the thermal performance of PCS walls. O'Hegarty *et al*. (2020) conducted an in-depth exploration into the thermal performance of thin precast concrete sandwich panels, utilizing finite element models to identify prevalent design characteristics and areas susceptible to heat loss, subsequently implementing measures to mitigate the thermal bridge effect. Hu *et al*. (2018a) embarked on finite element simulations to analyze the temperature field of precast sandwich insulated exterior wall panels, delving into the thermal bridges engendered by the installation of

window frames within prefabricated sandwich insulated exterior wall panels, all examined through the lens of ANSYS simulation. Employing the finite element temperature analysis module proves immensely advantageous in the study of wall thermal performance, with ANSYS serving as a widely embraced, comprehensive software boasting reliable simulation outcomes. However, research on the thermal performance of bamboo walls utilizing ANSYS is limited.

Research pertaining to the operational efficacy of bamboo assembled houses is currently underway. Sharma *et al*. (2015) examined the performance of engineered bamboo, engaging in discussions regarding potential limitations in structural design. Ultimately, they concluded that engineered bamboo products exhibit properties that are comparable to, if not surpassing, those of their timber and wooden counterparts. Hu *et al*. (2018b) fortified the bolted connection nodes in assembled round bamboo structures through the implementation of various treatments, including the utilization of single bolts, double bolts, and nodal domain high-strength mortar. Subsequent tests revealed a notable enhancement in performance post-strengthening. Xiao *et al*. (2009) employed bamboo plywood as the primary material in the design, processing, and installation of assembled bamboo houses. Through a combination of tests and theoretical analysis, they scrutinized and evaluated the operational efficacy of these assembled bamboo houses upon completion. Zhou *et al*. (2011) conducted fire tests on assembled bamboo houses, ultimately corroborating their superior fire resistance performance when compared to light steel plate houses. This begs the question: what about research dedicated to exploring the thermal performance of walls within bamboo assembled houses?

Drawing upon pre-developed panels and pertinent research, the present work employed the ANSYS finite element simulation method to simulate and examine the impact of thermal bridging on various structural components within the walls of bamboo assembled houses. This endeavor encompassed an analysis of the keel thickness, inner and outer walls, insulation layer, and other pertinent elements, all aimed at mitigating the adverse effects of thermal bridging. Consequently, a rational reference range for each thickness parameter was proposed, and subsequent resimulation was conducted to enhance the thermal performance of bamboo walls and minimize the occurrence of thermal bridging. Building upon this foundation, a comprehensive study was undertaken to evaluate the thermal performance of bamboo assembled house walls, employing an appropriate wall thickness. This entailed conducting surface temperature tests on both bamboo and iron walls within assembled houses, under real-world conditions, to validate the thermal insulation capabilities of bamboo walls. The findings of this study can serve as a reference for optimizing the design of thermal performance within bamboo assembled house walls.

EXPERIMENTAL

Finite-Element Modeling

Basic assumptions

To simulate the keel-added thermal bridges generated by the exterior walls, it is necessary to assume:

(1) Constant indoor and outdoor temperatures and no transient change in wall insulation performance with the external environment;
(2) Transformation of the three-dimensional problem into a two-dimensional problem, where only the heat transfer in the horizontal direction is studied;

(3) The parameters of each material in the insulation construction do not change with temperature;
(4) The model boundary conditions remain unchanged, *i.e.*, type 3 boundary conditions: the surface heat transfer coefficient and the corresponding temperature for a given model.
(5) Neglecting the impact of convective heat transfer from the indoor and outdoor environment on the simulation.

Parameter setting

A plane77 two-dimensional thermal solid unit in the ANSYS finite element program was selected to simulate the structural components of steel, bamboo board, and insulated asbestos walls, as shown in Fig. 1. Referring to the relevant material experimental data and GB 50176-2016 Thermal Design Code for Civil Buildings, from top to bottom, the main materials of the wall and their thermal conductivity are as follows: bamboo bundle veneer laminated material 0.0787 W/(m·K), rock wool 0.045 W/(m·K), and steel keel (stud) 58.2 W/(m·K). The winter thermal calculation parameters were selected as the simulation conditions, which were -3 °C outdoors and 18.0 °C indoors, and the left and right sides were set as adiabatic conditions; the boundary conditions were defined by convective heat flux, and the heat transfer coefficient was taken as 8.7 W/(m^2·K) for the inner surface and 23.0 W/(m^2·K) for the outer surface.

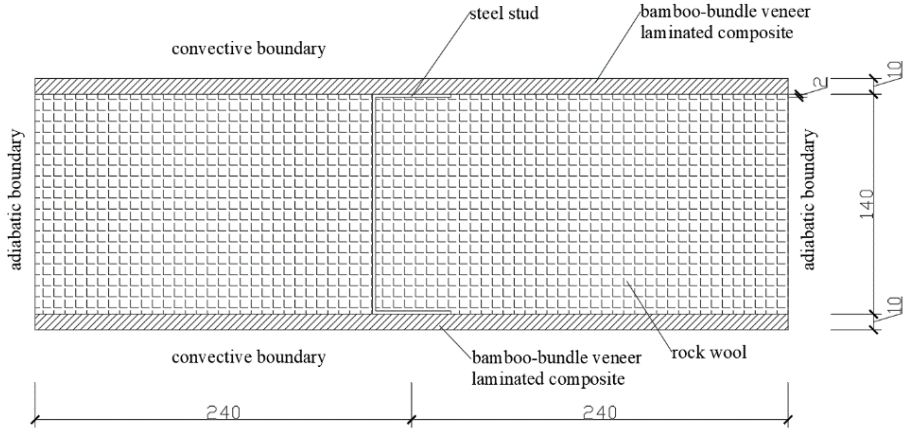

Fig. 1. The finite element model

Mesh division

After the geometric model is determined, the length of the divided mesh is set to 0.01 mm to enter the meshing stage as shown in Fig. 2, and the temperature field variation map is derived by loading the above parameters and boundary conditions. Enter the post-processing stage: export the relevant data for calculation.

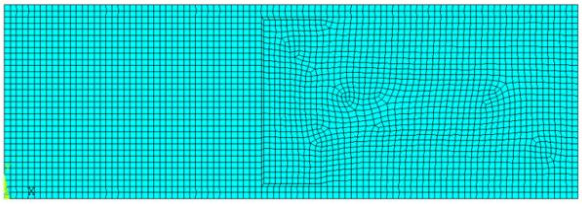

Fig. 2. Mesh subdivision

Theoretical analysis

ANSYS thermal analysis can perform finite element calculations on the temperature for each node. The differential equation for the steady state case is.

$$\frac{\partial}{\partial x}\left(\lambda_x \frac{\partial t}{\partial x}\right) + \frac{\partial}{\partial_y}\left(\lambda_y \frac{\partial_t}{\partial y}\right) + \Delta Q = 0 \quad (1)$$

The finite element equilibrium equation is,

$$[K]\{T\} = \{Q\} \quad (2)$$

where K is the conductivity matrix, T is the Node temperature vector, and Q is the Nodal heat flow rate vector.

The average heat transfer coefficient of the keel (stud) in the bamboo wall cannot be calculated by the formula of the average heat transfer coefficient of the wall because of its heat transfer does not have continuity, and the calculation method combined with software simulation results is used. According to the basic formula of heat transfer, the heat transfer coefficient of the wall is determined. The average heat flow density q of the wall can be calculated by ANSYS software simulation, and then the heat transfer coefficient of the wall is calculated as follows,

$$q = \frac{Q}{L} \quad (3)$$

where Q is total heat flow, obtained by integrating the heat flow density (W), and L is unit length (m),

$$\mathrm{R} = \frac{(T_1 - T_2)}{q}(T_1 > T_2) \quad (4)$$

$$\mathrm{R} = \Sigma_{\mathrm{i}} \frac{d_i}{\lambda_i} \quad (5)$$

$$R_0 = R_i + R + R_e \quad (6)$$

$$K_0 = \frac{1}{R_0} \quad (7)$$

where q is heat flow density (W/m^2), T is temperature (°C), R is wall heat transfer resistance (m^2·K/W), R_i is inner surface heat transfer resistance (m^2·K/W), R_e is external surface heat transfer resistance (m^2·K/W)W, R_0 is total thermal resistance of flat wall (m^2·K/W), and K_0 is total heat transfer coefficient of the flat wall [W/(m^2·K)]. The internal surface heat transfer resistance and external surface heat transfer resistance are 0.11 m^2·K/W and 0.04 m^2·K/W, respectively.

RESULTS AND DISCUSSION

Heat Transfer Analysis

Based on the insulation system of the wall of the assembly building system and the force characteristics of the bamboo wall, the wall model is established and three variables in the thickness of the inner wall panel, the thickness of the keel (stud), the thickness of the insulation layer, and the thickness of the outer wall panel are limited. The other variable is changed to explore the setting of the reasonable thickness of each part of the bamboo wall to mitigate the effect of thermal bridging, and the temperature field variation diagram

obtained is shown in Fig. 3. Through the model simulation, the temperature data are obtained, and then the heat transfer coefficient is calculated to achieve the purpose of analyzing the heat transfer of the wall.

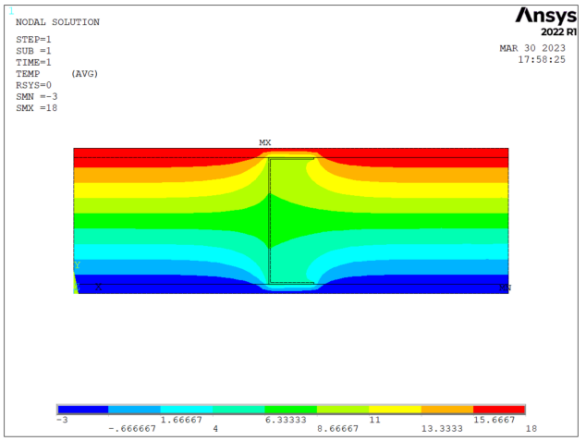

Fig. 3. Temperature field variation

Effect of Outer Panel Thickness

The thickness of the external wall panel is controlled as a single variable, the simulation is divided into five groups, and the thickness of the external bamboo panel is alternately set to 8, 10, 12, 15, and 20 mm. Other parameters are set as follows: keel flange width 50 mm, keel thickness 2 mm, insulation layer rock wool thickness 140 mm, keel spacing 480 mm, and internal panel thickness 10 mm.

Figure 4 shows the distribution of heat flow density along the X (unit wall length direction, length L = 0.48 m) direction for the experimentally used wall panel size, the line integration of heat flow density in the X direction is performed, and the total heat flow density Q=6.687 W/m^2 is obtained, as shown in Fig. 5. The heat transfer coefficient K_0=0.6275 W/(m^2·K) is obtained by substituting it into the above equation.

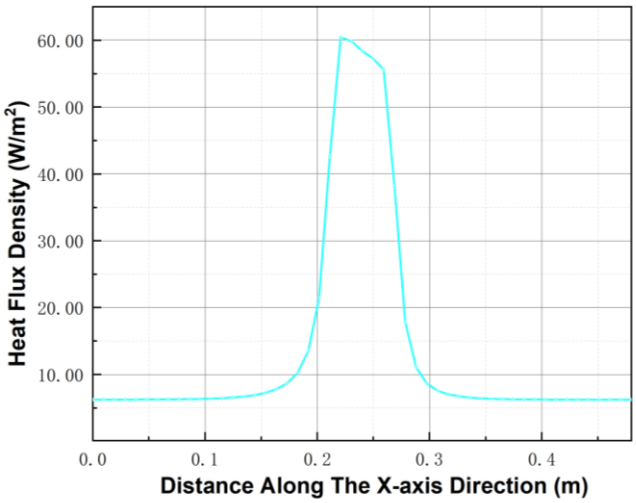

Fig. 4. The heat flux density diagram of the model along the X direction

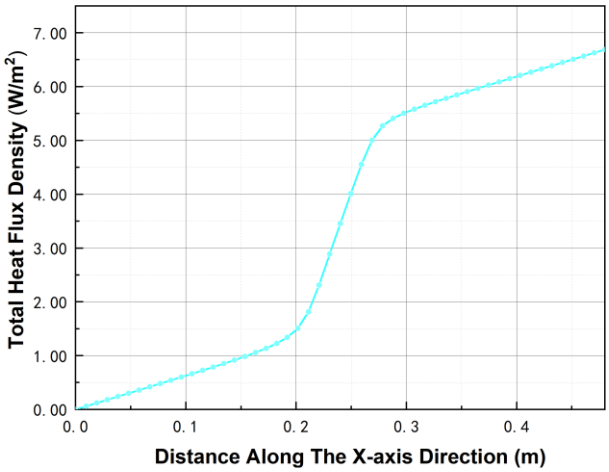

Fig. 5. The model integrates the total heat flux density along the X direction

The relevant calculation results, such as the heat transfer coefficient of the bamboo assembled house wall, are shown in Table 1, and the change trend of the heat transfer coefficient of the wall is shown in Fig. 7. The larger thickness of the exterior wall panel results in a smaller the heat transfer coefficient, but with the gradual increase in the thickness of the exterior wall panel, the curve tends to be smooth. The heat transfer coefficient of the wall increases 0.0805 W/(m^2·K) when the thickness of the exterior wall panel increases from 8 mm to 10 mm, and 0.1165 W/(m^2·K) when the thickness of the exterior wall panel increases from 10 mm to 12 mm. After the thickness of the exterior wall panel exceeds 15 mm, the change in the thickness of the exterior wall panel will have a smaller effect on the heat transfer coefficient of the wall. As shown in Fig. 4, the presence of steel in the middle leads to an uneven distribution of the wall, making it difficult to calculate its theoretical value of thermal resistance, and the temperature changes drastically in the steel keel region. The simulated edge heat transfer coefficient K_1 is calculated based on the simulated edge heat flow density, and the edge theoretical heat transfer coefficient K_2 is calculated based on the thermal resistance of each layer according to Eq. 5. Comparing the two values, it is found that the error is small, both within 3%, indicating that the simulation test results are reliable.

Table 1. Grouping Simulation Results for Different Thicknesses of Exterior Wall Panels

Thickness of external wall panels	8	10	12	15	20
Total heat flow density Q	6.9821	6.6870	6.4354	6.1186	5.7030
Temperature on the side of the keel near the inner wall T	9.538	10.157	10.394	10.913	11.535
Average heat flow density q	14.5459	13.9313	13.4070	12.7472	11.8813
Average heat transfer coefficient K_0	0.6275	0.6034	0.5826	0.5564	0.5215
Edge heat flow density q_1	6.3388	6.2498	6.1664	6.0494	5.8696
Edge heat transfer coefficient K_1	0.2888	0.2849	0.2813	0.2761	0.2683
Theoretical edge K_2	0.2865	0.2845	0.2824	0.2794	0.2746
K_1 and K_2 errors	0.77%	0.15%	0.42%	1.18%	2.29%

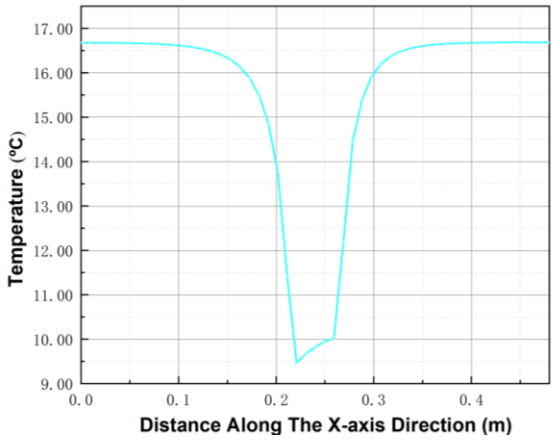

Fig. 6. The temperature distribution of the outer panel along the steel keel side

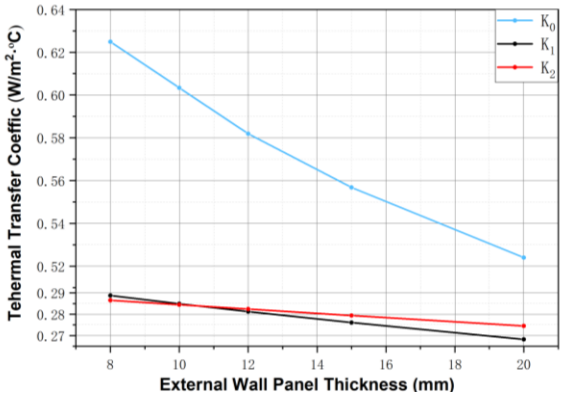

Fig. 7. The influence of the thickness of the outer wall on the heat transfer coefficient

The lowest temperatures of each group of simulated keels near the inner wall panel side are 9.5, 10.2, 10.4, 10.9, and 11.5 °C. The lowest temperature of the keel near the inner wall panel side gradually increases, the temperature difference between the keel and wall decreases, and the thermal bridge effect is weakened. A comprehensive comparison of the simulation results shows that the smaller the thickness of the exterior wall is, the more concentrated the heat transfer parts are, resulting in low internal wall temperature and easy formation of condensation, but the increase in the thickness of the exterior wall panel will also lead to an increase in the wall affected by the thermal bridge range. Therefore, the thickness of the external wall panel should be taken as a moderate value, not too large or too small.

Effect of Keel Thickness

The control keel thickness is a single variable, and the simulation is divided into five groups with keel thicknesses of 1, 1.5, 2, 2.5, and 3 mm. Other parameters are set as follows: insulation thickness of 140 mm, keel spacing of 480 mm, exterior panel thickness of 10 mm, and interior panel thickness of 10 mm.

Results are shown in Fig. 8. The heat transfer coefficient of the wall becomes larger, and with the increase in the keel thickness, the increase in the heat transfer coefficient of the wall decreases, and the change in the keel thickness has very little effect on the edge heat transfer. The difference between the theoretical calculation and the simulation results is less than 0.001, and the simulation results are reliable.

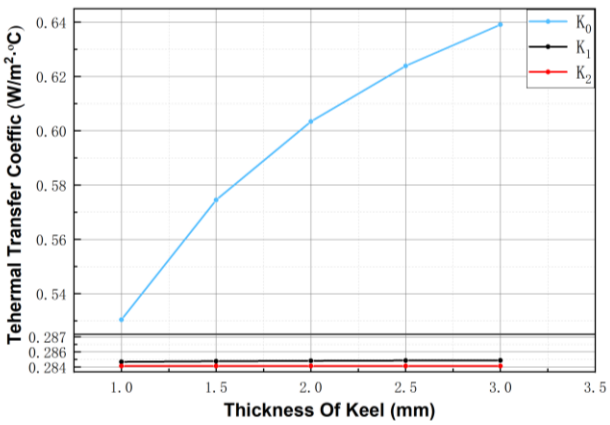

Fig. 8. Influence of keel thickness on heat transfer coefficient

The simulated wall temperature distribution shows that the minimum temperature of the keel near the inner wall side is 11.5, 10.7, 10.2, 9.7, and 9.4 °C with increasing keel thickness, and the minimum temperature of the keel near the inner wall side is gradually reduced. When the keel thickness was increased from 1 to 1.5 mm, the minimum temperature of the keel near the inner wall side decreased by 0.8 °C, and when the keel thickness was increased from 2.5 to 3 mm, the minimum temperature of the keel near the inner wall side decreased by 0.3 °C. With the gradual increase in the keel thickness, the effect of the keel thickness on the minimum temperature of the keel near the inner wall side gradually decreased. At the same time, with the increase in keel thickness, the influence range of the thermal bridge accordingly becomes larger. A comprehensive comparison of the simulation results shows that as the thickness of the keel increases, the lower the temperature of the keel near the inner wall side, the more concentrated the heat flow is, the more obvious the thermal bridge effect is, and the more likely condensation is to occur.

As shown in Figs. 5 and 6, in the area where the steel keel is present, the heat flow density increases significantly, the thermal bridge effect is significant, the temperature curve at the measurement point at the combined keel fluctuates the most, the heat transfer process is obvious, and the insulation performance is the worst. The steel keel with the highest thermal conductivity is obviously the main component causing thermal bridging. To quantitatively study the effect of the steel keel on the heat transfer coefficient of the bamboo wall, finite element models with keel steel plate thicknesses of 1, 1.5, 2, 2.5, and 3 mm were used, and the heat transfer coefficient was plotted against the thickness of the central steel plate keel, as shown in Fig. 8. It was noted that the heat transfer coefficient of the wall increased almost linearly as the keel thickness increased, and by increasing the keel thickness from 1 to 3 mm, the heat transfer coefficient increased by 20.49%. Therefore, reducing the keel thickness can significantly improve the thermal performance of bamboo house walls.

In summary, whether it is to reduce the effect of thermal bridging or to improve the thermal performance of the wall, the keel thickness should not be too high and should be reduced appropriately.

Effect of Insulating Layer Thickness

With the insulation thickness controlled as a single variable, the simulation is divided into five groups, and the keel heights are 100, 120, 140, 160, and 180 mm. Other

parameters are set as follows: keel thickness 2 mm, keel spacing 480 mm, external panel thickness 10 mm, and internal panel thickness 10 mm.

The results are shown in Fig. 9. The heat transfer coefficient of the wall decreases, and with the increase in the height of the insulation layer, the reduction in the heat transfer coefficient of the wall decreases, and the theoretical calculation and the simulated heat transfer situation basically remain consistent, which is influenced by the thickness of the insulation layer.

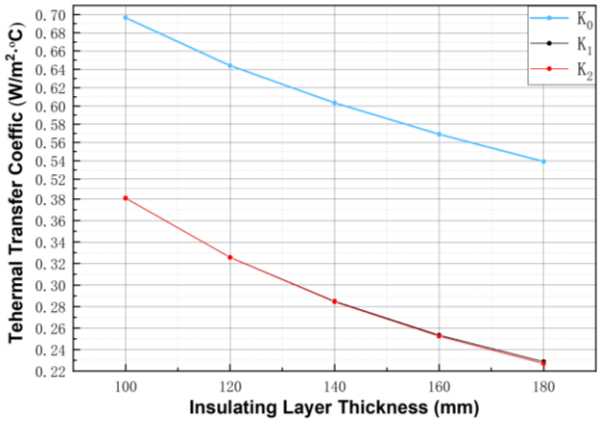

Fig. 9. The effect of insulation thickness on heat transfer coefficient

From the wall temperature distribution diagram, it can be seen that with increasing insulation thickness, the lowest temperatures of the keel near the inner wall side in the simulation are 9.3, 9.7, 10.2, 10.3, and 10.5 °C, and the lowest temperature of the keel near the inner wall side gradually increases. A comprehensive comparison of the simulation results shows that the smaller the thickness of the insulation layer is, the lower the temperature on the side of the keel near the inner wall, and the more obvious the thermal bridge phenomenon, which may cause condensation. With the increase in the insulation layer thickness, the heat transfer coefficient almost linearly decreases; from 100 mm thick to 180 mm, the heat transfer coefficient decreases by 29.63%, but its decreasing trend is slowing down.

In summary, increasing the thickness of the insulation layer of the wall's overall insulation performance becomes stronger, to a certain extent to reduce the thermal bridge effect on the wall. Continuing to increase the thickness of the insulation rock wool will also improve the thermal performance of the wall, but with the increase in cost at the same time, the effect is weakened and should be based on the actual situation to choose the appropriate thickness of the insulation layer.

Effect of Inner Panel Thickness

Controlling the thickness of the inner wall panel as a single variable, the simulation was divided into five groups, and the thickness of the outer bamboo wall panel was 8, 10, 12, 15, and 20 mm. Other parameters were set as follows: keel flange width 50 mm, keel thickness 2 mm, insulation layer rock wool thickness 140 mm, keel spacing 480 mm, and outer panel thickness 10 mm.

The results are shown in Fig. 10. The heat transfer coefficient of the wall tends to decrease, and as the thickness of the inner wall panel increases, the heat transfer coefficient of the wall decreases less and less, and the error between K_1 and K_2 is small and in a reasonable range.

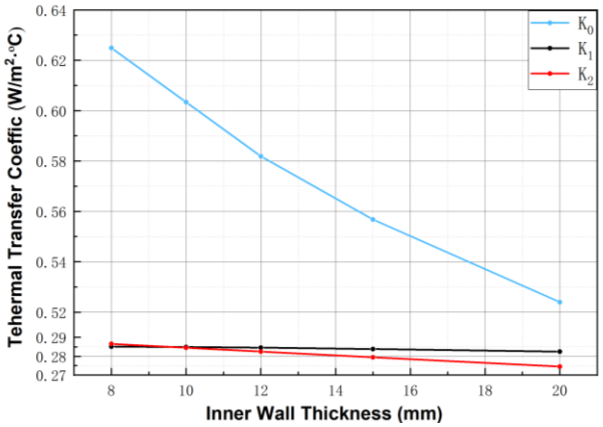

Fig. 10. The influence of inner wall thickness on heat transfer coefficient

The simulated wall temperature distribution shows that the minimum temperature of the keel near the inner wall side decreases gradually as the thickness of the inner wall panel increases: 10.8, 10.1, 9.3, 8.5, and 7.6 °C. When the thickness of the inner wall panel was increased from 8 mm to 10 mm, the minimum temperature of the keel near the inner wall side decreased by 0.7 °C, and when the thickness of the inner wall panel increased from 10 mm to 12 mm, the minimum temperature of the keel near the inner wall side decreased by 0.8 °C. With the gradual increase in the thickness of the inner wall panel, the effect of the thickness of the inner wall panel on the minimum temperature of the keel near the inner wall side gradually became larger. With the increase in the thickness of the inner wall panel, the influence range of the thermal bridge also became slightly larger. Through the comprehensive comparison of the simulation results, it can be seen that with the increase in the thickness of the inner wall board, the lower the temperature of the keel near the inner wall side, the more concentrated the heat flow, the more obvious the thermal bridge effect, and the more likely condensation occurs, resulting in moisture in the box insulation material and further damage to the insulation system of the box. However, with the increase in the thickness of the inner wall panel, the heat transfer coefficient is also reduced accordingly, enhancing the thermal insulation performance of the wall.

In summary, in the case of ensuring the structural performance, it is recommended to choose a more appropriate thickness of the inner wall panels, that is, to reduce the impact of the thermal bridge effect but also to ensure its thermal performance.

Optimized Design of Bamboo Wall Heat Transfer

The comprehensive research described above showed that the heat transfer coefficient of the wall decreases with increasing thickness of the inner and outer wall panels and insulation layer, while it is inversely proportional to the thickness of the keel. To further optimize the heat transfer of the bamboo wall, the range of wall thicknesses commonly used for load-bearing and self-bearing exterior walls is combined with the climatic differences between northern and southern China, and the thickness specification of the 160 mm wall is selected by drawing on the standard of steel and wood doorways. The thermal bridge influencing factors include the thickness of the inner and outer wall panels, the thickness of the insulation layer, keel thickness, keel material, *etc.* For the combination of program design and calculation, the results are shown in Table 2.

The comparison of scheme $1^{\#}$ and $2^{\#}$ shows that the thickness of the steel keel is reduced by only 1 mm, and its heat transfer coefficient is reduced by 0.0455 W/(m^2·K);

comparing scheme 2# and 3# shows that the total thickness of the inner and outer wall panels is increased by 4 mm, the thickness of the insulation layer is reduced by 4 mm, and its heat transfer coefficient is reduced by 0.04 W/(m^2·K); comparing scheme 3# and 4#, the total thickness of the inner and outer wall panels is increased by 10 mm, the thickness of the insulation layer is reduced by 10 mm, and the heat transfer coefficient is reduced by 0.04 W/(m^2·K). The heat transfer coefficient is reduced by 0.0686 W/(m^2·K) when the insulation layer thickness is reduced by 10 mm, which is a significant improvement compared with the previous 2# and 3#; while the comparison of scheme 4# and 5# reveals that the heat transfer coefficient is reduced by 0.0177 W/(m^2·K) when the thickness of the steel keel is continuously reduced on the basis of 4#, which has a decreasing trend compared with the previous improvement in thermal performance; it can be found that the thermal performance is affected by the steel keel thickness. Although the volume of the light steel keel accounted for a small percentage, its thermal conductivity was great. To further consider the impact of the keel, the light steel keel was replaced with wood keel to form program 6#, where the glued wood thermal conductivity of 0.17 W/(m·K), similar to bamboo, reducing the thermal bridge effect between the two. Compared to 5# heat transfer coefficient is reduced by 0.222 W/(m^2·K); however, in order to increase structural stability, the wood keel thickness of 20 mm or more suitable, forming program 8#, compared to 7# wood keel thickness increased to 20 mm, the heat transfer coefficient increased by 0.0289 W/(m^2·K), verifying the greater impact of steel keel thickness on thermal performance.

After the above analysis, the average heat transfer coefficient of scheme 5# after thickness optimization is nearly 25% smaller than that of scheme 1#, the influence range of the thermal bridge is relatively reduced, and the thermal performance of the bamboo wall is enhanced. After using wood keel instead of steel keel, the heat transfer coefficient shrinks significantly to 0.2222 W/(m^2·K), compared with the thickness optimization before the thermal performance is improved by nearly 100%, a significant improvement. The impact of wood keel thermal bridge is shown in Fig. 11 and Fig. 12. The bamboo and wood thermal conductivity is relatively close, the temperature in the two connection areas there is a temperature change, but only in 0.5 °C, there is almost no thermal bridge effect problem. The comparison of scheme 1# and 2# shows that the thickness of steel keel is reduced by only 1mm, and its heat transfer coefficient is reduced by 0.0455 W/(m^2·K); comparing scheme 2# and 3# shows that the total thickness of inner and outer wall panels is increased by 4 mm, and the thickness of insulation layer is reduced by 4 mm, and its heat transfer coefficient is reduced by 0.04 W/(m^2·K); comparing scheme 3# and 4#, the total thickness of inner and outer wall panels is increased by 10 mm, and the thickness of insulation layer is reduced by 10 mm, and the heat transfer coefficient is reduced by 0.04 W/(m^2·K). The heat transfer coefficient is reduced by 0.0686 W/(m^2·K) when the insulation layer thickness is reduced by 10 mm, which is a significant improvement compared with the previous 2# and 3#; while the comparison of scheme 4# and 5# reveals that the heat transfer coefficient is reduced by 0.0177 W/(m^2·K) when the thickness of steel keel is continuously reduced on the basis of 4#, which has a decreasing trend compared with the previous improvement of thermal performance. It can be found that the thermal performance is affected by the steel keel thickness is the most affected. Although the volume of the light steel keel accounted for a small percentage, but its thermal conductivity is great, in order to further consider the impact of the keel, so remove the light steel keel replaced with wood keel to form program 6#, where the glued wood thermal conductivity of 0.17 W/(m·K), similar to the bamboo, reducing the thermal bridge effect between the two, compared to 5# heat transfer coefficient is reduced by 0.222 W/(m^2·K). However, in

order to increase the structural stability, the wood keel thickness of 20 mm or more suitable, forming program 8#, compared to 7# wood keel thickness increased to 20 mm, the heat transfer coefficient increased by 0.0289 W/(m^2·K), verifying the greater impact of steel keel thickness on thermal performance.

Table 2. Calculated Results after Optimization

Number	Program Design (Thickness:160 mm)				Average heat transfer coefficient K_0 / W/(m^2·K)
	Thickness of internal and external wall panels (mm)	Insulation Thickness (mm)	Keel		
			Material	Thickness (mm)	
1#	8	144	steel	3	0.6889
2#	8	144	steel	2	0.6434
3#	10	140	steel	2	0.6034
4#	15	130	steel	2	0.5348
5#	15	130	steel	1.5	0.5171
6#	15	130	wood	1.5	0.2949
7#	10	140	wood	2	0.2879
8#	10	140	wood	20	0.3168

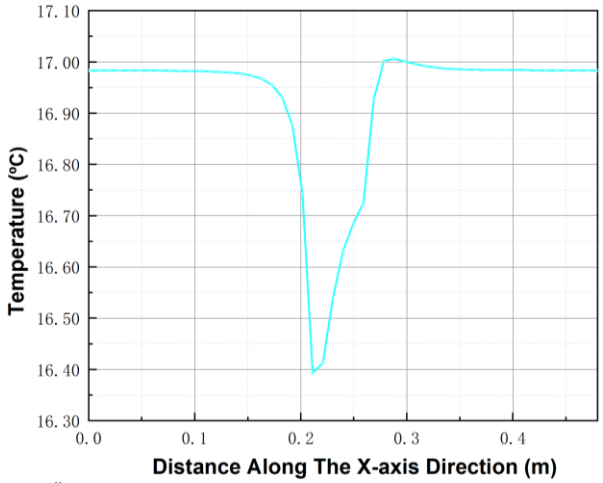

Fig. 11. Temperature of 7# keel along one side of the interior wall

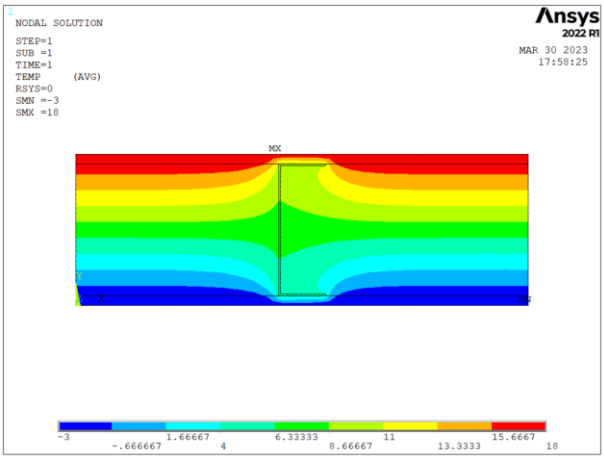

Fig. 12. 7# Temperature field variation diagram

Thermal Performance Testing of Bamboo Assembled House Walls

The simulation analysis reveals that modulating the thickness of the internal and external wall panels, framework, and insulation layer can effectively enhance the thermal insulation performance of bamboo walls while mitigating the thermal bridging effect. This serves as a foundational reference for practical implementation. Taking into consideration the robustness of the bamboo and wood structure, as well as the connectivity of its junctions and ease of assembly, the 3# and 8# solutions, embodying moderate thermal performance, secure connections, and lightweight attributes, were chosen for experimental evaluation. Drawing inspiration from the numerical simulation study, two containerized dwellings were constructed for this investigation. One is a conventional iron-constructed assembly (referred to as "iron"), while the other is a bamboo bundled veneer wall assembly (referred to as "bamboo"), crafted utilizing the research group's findings. Both houses possess identical dimensions and spatial layouts, permitting temperature tests to be conducted on their internal and external surfaces, thereby elucidating the distinctive characteristics of bamboo-constructed walls in house building.

Temperature Collection on the Internal and External Surfaces of the Wall

The experimental site is situated in Galutu town, Wushen Banner, Ordos City, Inner Mongolia (38.60°N, 108.84°E). Figure 13 visually depicts two south-facing boxes, measuring 12 meters in length and 2.4 m in width. The bamboo wall is designed to have a thickness of 160 mm, consisting of 10 mm thick inner and outer wall panels, with an insulation layer measuring 140 mm in thickness. In comparison, the iron wall represents a conventional container wall, possessing the same thickness as the bamboo wall. A comprehensive study and comparison between the two walls was conducted. During the test, the weather conditions were sunny, and no heating or air conditioning was employed within the room. Solar radiation served as the primary source of heat within the space. The distribution of test points is illustrated in Fig. 14. The research team utilized Hangzhou Luger temperature recorders to collect data on wall surface temperature and indoor temperature. Each temperature meter employed was a four-channel tester with a measurement accuracy of ±0.5 °C. The test points were positioned at a height of 1.8 m from the floor, with temperature meters arranged on the south and north walls of the house. The primary focus of the tests encompassed the indoor temperature, as well as the internal and external surface temperatures of the north and south interior and exterior walls. And the coldest time area is selected as the Major Cold, which lasted for 5 days, and the test instrument recorded the data automatically every 30 min.

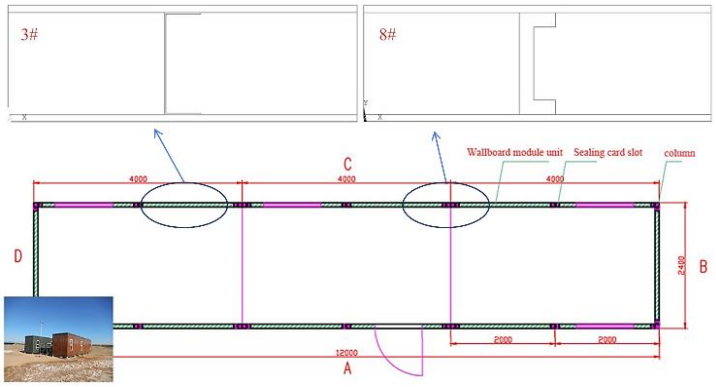

Fig. 13. Test environment and building plan

Fig. 14. Temperature measuring point position

Temperature Analysis Inside and Outside the Wall

Temperature records are shown in Fig. 15. The temperature of the inner and outer surface of the wall varied greatly. The temperature of the outer surface of the south-facing wall was higher than the temperature of the inner surface. The temperature difference between the inner and outer surface was large, the maximum temperature difference of the iron test reached 35.1°C, and the temperature difference of bamboo was 26.1°C. This is because the south-facing balcony receives sunlight immediately after sunrise, the indoor air warms up rapidly during the day, and the thermal inertia of the wall makes the inner wall have a smaller change in surface temperature than that of the outer surface. Similar to the south-facing wall, the temperature change trend of the inner and outer surface of the north-facing wall was similar, but the temperature difference between the inner and outer surface was smaller than that of the south-facing, with a temperature difference of approximately 4 to 5 °C, and the change in the iron temperature difference was also larger than that of bamboo. The difference is that the north-facing wall cannot receive sunlight, so the north-facing wall cannot be heated directly by the sun, resulting in a lower temperature on the outside surface of the wall than the indoor temperature, and the temperature difference is reduced accordingly.

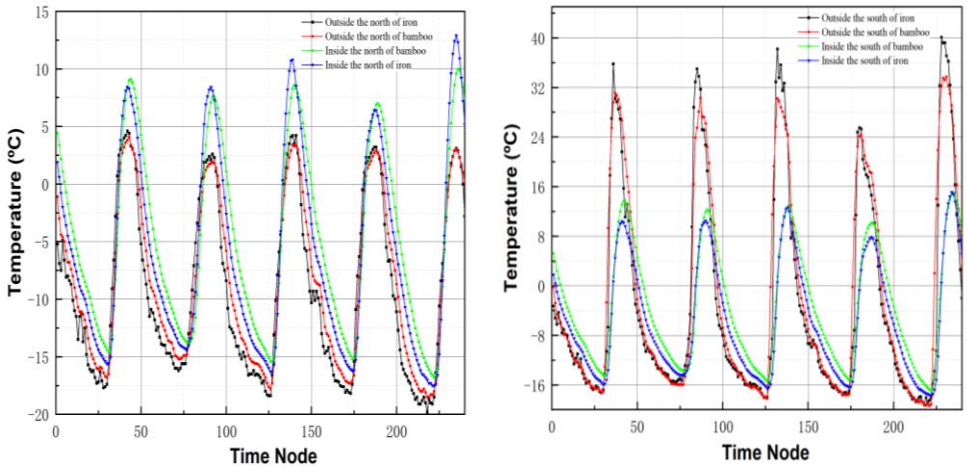

Fig. 15. Temperature data processing (left-south, right-north)

In the rising temperature stage, the trends of bamboo and iron were basically the same, but in the decreasing temperature stage, the temperature decreasing trend of bamboo was slower than that of iron. At the same time, when the outdoor temperature began to decrease, the indoor temperature of bamboo wall houses began to decrease slowly, while the indoor temperature decrease rate of traditional iron container type houses was significantly higher than that of bamboo. In terms of the temperature difference and temperature drop rate, bamboo was smaller than iron, which shows that bamboo walls had a larger thermal inertia index and stronger heat storage capacity. Therefore, bamboo walls are more suitable for use and promotion in desert microenvironments than traditional iron walls.

CONCLUSIONS

1. The simulation results unveiled a substantial temperature gradient and heat flux in proximity to the steel keel (stud). As the keel thickness increases, the area impacted by thermal bridging expands, signifying a prominent thermal bridging effect within the keel region. Thus, efforts to mitigate thermal bridging should concentrate on the keel area.
2. The heat transfer coefficient diminishes as the thickness of the exterior wall panel, insulation layer, and interior wall panel increases, thereby enhancing the thermal performance of the bamboo wall. Conversely, an increase in keel thickness correlates with a higher heat transfer coefficient, thus weakening its thermal performance.
3. The optimized bamboo wall exhibits improved thermal performance and diminished thermal bridging. Remarkably, the substitution of steel keels with wooden counterparts yields a particularly noteworthy outcome, reducing the heat transfer coefficient by approximately twofold and mitigating the effects of thermal bridging. Consequently, the preference should be given to employing wooden keels.
4. The test results affirm that, when considering all factors, a bamboo wall, as specified in this work, attenuates the impact of outdoor temperature on indoor temperature. Displaying heightened thermal inertia and superior thermal storage capacity, the bamboo wall exhibits commendable thermal performance.

ACKNOWLEDGMENTS

This work was financially supported by the Natural Science Foundation of Henan Province (222300420162), the Key R&D and Promotion Special Project of Henan Province (Science and Technology Targeting) (212102310960), the Key Scientific Research Project of Higher Education in Henan Province (18A220001), the PhD Foundation of Henan Polytechnic University (B2017-39), and the Innovation and Entrepreneurship Program for College Students in Henan Province (202210460060). Finally, we would like to thank undergraduate student Jiayi Hao for her efforts in the early project research.

REFERENCES CITED

Alghamdi, A. A., and Alharthi, H. A. (2017). "Multiscale 3D finite-element modelling of the thermal conductivity of clay brick walls," *Construction and Building Materials* 157, 1-9. DOI: 10.1016/j.conbuildmat.2017.09.081

Chen, F., Jiang, Z., Deng, J., Wang, G., Zhang, D., Zhao, Q., Cai, L., and Shi, S. Q. (2013). "Evaluation of the uniformity of density and mechanical properties of bamboo-bundle laminated veneer lumber (BLVL)," *BioResources* 9(1), 554-565. DOI: 10.15376/biores.9.1.554-565

Hu, C., Li, X., He, X., and Song, T. (2018a). "Finite element analysis of the temperature field of the insulated wall panel," *Building Science* 34(02), 74-82.

Hu, H., Yang, J., Wang, F., and Zhang, Y. (2018b). "Mechanical properties of bolted joints in prefabricated round bamboo structures," *Journal of Forestry Engineering* 3(05), 128-135.

Huang, Z., and Sun, Y. (2021). "Hygrothermal performance comparison study on bamboo and timber construction in Asia-Pacific bamboo areas," *Construction and Building Materials* 271, article 121602. DOI: 10.1016/j.conbuildmat.2020.121602

Huo, H., Shao, J., and Huo, H. (2017). "Contributions of energy-saving technologies to building energy saving in different climatic regions of China," *Applied Thermal Engineering* 124, 1159-1168. DOI: 10.1016/j.applthermaleng.2017.06.065

Li, Y., Shan, W., Shen, H., Zhang, Z.-W., and Liu, J. (2015). "Bending resistance of I-section bamboo-steel composite beams utilizing adhesive bonding," *Thin-Walled Structures* 89, 17-24. DOI: 10.1016/j.tws.2014.12.007

Li, Y., Yao, J., Li, R., Zhang, Z., and Zhang, J. (2017). "Thermal and energy performance of a steel-bamboo composite wall structure," *Energy and Buildings* 156, 225-237. DOI: 10.1016/j.enbuild.2017.09.083

Liu, J., Sun, C., Zhao, S., and Li, Y. (2022). "Simulation of thermal performance of composite insulated blocks with recycled aggregate concrete," *Concrete* (8), 119-124.

Lv, Q., Wang, W., and Liu, Y. (2019). "Study on thermal insulation performance of cross-laminated bamboo wall," *Journal of Renewable Materials* 7(11), 1231-1250. DOI: 10.32604/jrm.2019.08345

O'Hegarty, R., Reilly, A., West, R., and Kinnane, O. (2020). "Thermal investigation of thin precast concrete sandwich panels," *Journal of Building Engineering* 27, article 100937. DOI: 10.1016/j.jobe.2019.100937

Shan, Q., Tong, K., Zhang, X., and Li, Y. (2020). "Field test and simulation analysis of thermal performance of bamboo steel composite wall in different climate regions," in: *Advances in Civil Engineering*, M.-J. He (ed.), 2020, pp. 1-10. DOI: 10.1155/2020/8854156

Sharma, B., Gatoo, A., Bock, M., and Ramage, M. (2015). "Engineered bamboo for structural applications," *Construction and Building Materials* 81, 66-73. DOI: 10.1016/j.conbuildmat.2015.01.077

Trujillo, D. J. A., and Malkowska, D. (2018). "Empirically derived connection design properties for Guadua bamboo," *Construction and Building Materials* 163, 9-20. DOI: 10.1016/j.conbuildmat.2017.12.065

Xiao, Y., She, L., Shan, B., Zhou, Q., Yang, R., and Chen, G. (2009). "Research and design of prefabricated bamboo house," *Industrial Construction* 39(01), 56-59.

Yan, D., Hong, T., Li, C., Zhang, Q., An, J., and Hu, S. (2017). "A thorough assessment of China's standard for energy consumption of buildings," *Energy and Buildings* 143,

114-128. DOI: 10.1016/j.enbuild.2017.03.019
Yang, Z., Sun, L., Nan, B., and Wei, S. (2023). "Thermal performance of slotted light steel-framed composite wall," *Energies* 16(5), article 2482. DOI: 10.3390/en16052482
Zhai, X., Wang, Y., and Wang, X. (2018). "Thermal performance of precast concrete sandwich walls with a novel hybrid connector," *Energy and Buildings* 166, 109-121. DOI: 10.1016/j.enbuild.2018.01.070
Zhou, Q., She, L., Xiao, Y., Shan, B., Huo, J., Ma, J., and Yang, R. (2011). "Fire-resistance simulation and test of prefabricated bamboo house," *Journal of Building Structures* 32(7), 60-65+100.
Zhou, H., Sun, F., Li, H., Zhang, W., Cheng, H., Chen, L., Yu, Z., Chen, F., and Wang, G. (2019). "Development and application of modular bamboo-composite wall construction," *BioResources* 14(3), 7169-7181. DOI: 10.15376/biores.14.3.7169-7181
Zhou, X., Liu, F., and Ding, X. (2020). "Thermal insulation performance determination and performance optimization of composite wall with straw board," *New Building Materials* 47(5), 58-62.
Zhou, Q., Li, W., Tian, J., Liu, P., Jiang, N., and Fu, F. (2023). "Study on axial compression performance of original bamboo-fiber reinforced phosphogypsum composite walls," in: *Mechanics of Advanced Materials and Structures*, Taylor & Francis Inc, Philadelphia. DOI: 10.1080/15376494.2023.2192710

Article submitted: August 12, 2023; Peer review completed: November 4, 2023; Revised version received: November 11, 2023; Accepted: November 12, 2023; Published: November 21, 2023.
DOI: 10.15376/biores.19.1.416-433